Supplementary Material for "PAR-3 oligomerization may provide an actin-independent mechanism to maintain distinct Par protein domains in the early *C. elegans* embryo"

AT Dawes and EM Munro

Parameter	Meaning	Units
k_{on}^{A}	rate of ParA cortical association	s^{-1}
k_{off}^{A}	rate of ParA cortical dissociation	s^{-1}
k_c	rate of cytoplasmic ParA dimer formation	$\mu M^{-1}\ s^{-1}$
k_d^+	rate of ParA dimer formation	$\mu M^{-1}\ s^{-1}$
k_d^-	rate of ParA dimer break up	s^{-1}
r_A	rate of ParA phosphorylation by ParPs	$\mu M^{-1}\ s^{-1}$
$k_{on}^{A_{11}}$	rate of cortical association of second ParA in singly bound dimer	s^{-1}
k_{on}^{P}	rate of ParP cortical association	s^{-1}
k_{off}^{P}	rate of ParP cortical dissociation	s^{-1}
r_P	rate of ParP phosphorylation by ParAs	$\mu M^{-1}\ s^{-1}$
D_a, D_p	diffusion rate of ParA/ParP	$\mu m^2/s$
L	typical length of embryo	μm

Table S1: Dimensional parameters used in Equations 1.

Although the main focus of this work is on Par protein dynamics in the absence of an asymmetrically distributed actomyosin cortex, we also explored the consequences of coupling our Par protein model to the actomyosin model proposed by Tostevin and Howard (Tostevin and Howard, 2008). We use Equations (2)-(5) from that paper to simulate cortical actomyosin dynamics coupled to our Par protein model above, using a to denote the amount of cortical actomyosin, consistent with their notation.

Following Tostevin and Howard (2008), we modify the equations for A_1 and A_{10} such that a proportion of their cortical binding terms depend on the

Parameter	Definition	Value	Range
β_1	k_{on}^A/k_{off}^A	0.03	0.01-1
β_2	$k_d^+ A_y/k_{off}^A$	18.4	1-100
β_3	k_d^-/k_{off}^A	8.7	1-100
β_4	$r_A P_y/k_{off}^A$	12.8	1-100
β_5	$k_c A_y$	0.03	0.01-1
β_6	$k_{on}^{A_{11}}/k_{off}^A$	2.9	1-100
β_7	k_{on}^P/k_{off}^A	1	
β_8	k_{off}^P/k_{off}^A	1	
β_9	$r_P A_y/k_{off}^A$	72.5	1-100
α_y		1	
ρ_y		1	
D_1	$D_a/k_{off}^A L^2$	0.008	
D_2	$D_p/k_{off}^A L^2$	0.004	

Table S2: Non-dimensional parameters used in Equations 2 in terms of dimensional parameters, values used in this investigation, and the range of values used in the random parameter search.

concentration of cortical actomyosin:

$$\begin{aligned}\frac{\partial A_1}{\partial t} &= (0.9\beta_1 + 0.1\beta_1 a)\alpha_y - A_1 - 2\beta_2 A_1^2 + 2\beta_3 A_{11} - (0.9\beta_2 + 0.1\beta_2 a)\alpha_y A_1 \\ &\quad +\beta_3 A_{10} - \beta_4 P \cdot A_1 + D_1 \frac{\partial^2 A_1}{\partial x^2} \qquad \text{(S1a)} \\ \frac{\partial A_{10}}{\partial t} &= (0.9\beta_5 + 0.1\beta_5 a)\alpha_y^2 - A_{10} + (0.9\beta_2 + 0.1\beta_2 a)\alpha_y A_1 - \beta_3 A_{10} \\ &\quad -\beta_6 A_{10} + A_{11} - \beta_4 P \cdot A_{10} + D_1 \frac{\partial^2 A_{10}}{\partial x^2} \qquad \text{(S1b)}\end{aligned}$$

When we simulate this hybrid model, we find the model cell is able to polarize (Figure S2), and that the boundary between the Par protein domains stabilizes at a fixed position. This suggests that weak binding to polarized actomyosin plus positive feedback of ParA onto actomyosin contractility is sufficient to stabilize the AP boundary against drift.

When we deplete ParA in the hybrid model, there is a sudden loss of polarization (Figure S3, top two rows) in agreement with the actomyosin

Depletion factor	Fraction of parameters yielding successful solutions	% of successful solutions that are absolutely stable
Quasi-steady state	1/239066	0
$\alpha = 0.02$	1/230656	0
$\alpha = 0.05$	1/47608	10
$\alpha = 0.1$	1/4180	83

Table S3: Depletion of cytoplasmic pools can stabilize the AP boundary against drift. Parameter space searches were run under identical conditions for identical ranges of parameter values, but for different values of the depletion factor α. Note the sharp increase in the fraction of parameter sets yielding successful solutions and a stable AP boundary as α is increased from 0.02-0.1.

independent model. However, in contrast to what we observe with the actin independent model, depletion of ParP does not result in a loss of polarization (Figure S3, bottom two rows). Lowering both the cytoplasmic ParA and ParP allows the model to polarize again (Figure S4), in agreement with the results in the main text. In summary, adding the actomyosin model results in few changes to the results presented in the main text, with the exception of stabilizing the AP boundary against drift.

References

F Tostevin and M Howard. Modelling the establishment of PAR protein polarity in the one-cell C. elegans embryo. *Biophysical Journal*, 95(10), Jul 2008.

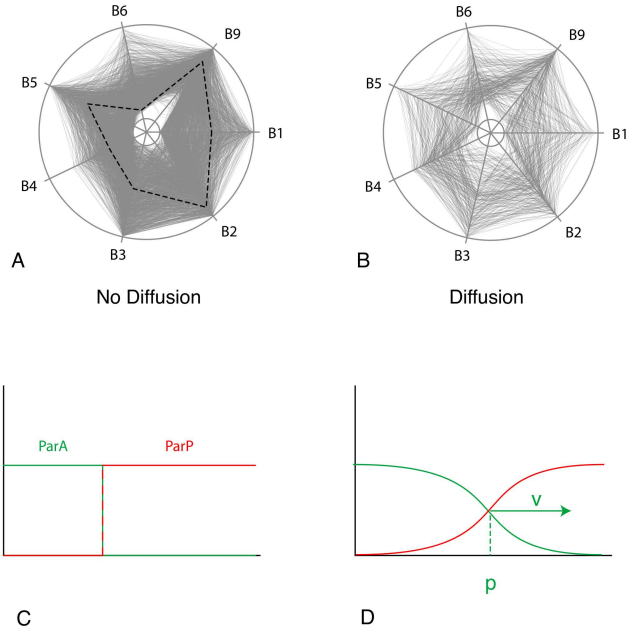

Figure S1: "Cam diagrams" showing distributions of parameter sets for which simulations stabilized complementary Par domains without (A) and with (B) diffusion. Each parameter set is represented as a polygon whose intersections with radial spokes indicate values for each parameter. Values range logarithmically from low near the cam center to high at its periphery. Initial conditions for each simulation are shown in panel C. For each choice of parameters, we tracked the ParA boundary (defined as the position where ParA concentration falls to half its maximum level; shown as "p" in panel D) and scored parameters as a success if the boundary speed fell below a threshold level of 1μm per five minutes and then remained below that threshold for an additional 100 time units.

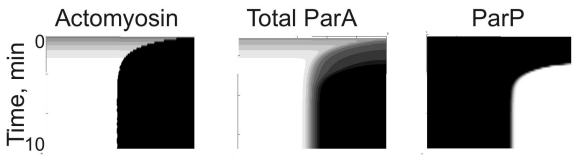

Figure S2: Par protein dynamics coupled to a model of the actin cortex from Tostevin and Howard (Tostevin and Howard, 2008). The initial stages of polarization are driven by active contraction of actomyosin towards the posterior pole to create a region of enhanced binding for ParA. Once established, the boundary between the anterior and posterior Par protein domains is buffered against drift by the enhanced binding of ParA to asymmetrically localized actomyosin, whose distribution is stabilized (as in Tostevin and Howard) by actomyosin contraction against an elastic resistance. Parameters used in the simulations are the same as those given in (Tostevin and Howard, 2008), with the exception of $\lambda_1 = 10$. Colormap legend is shown in Figure S3.

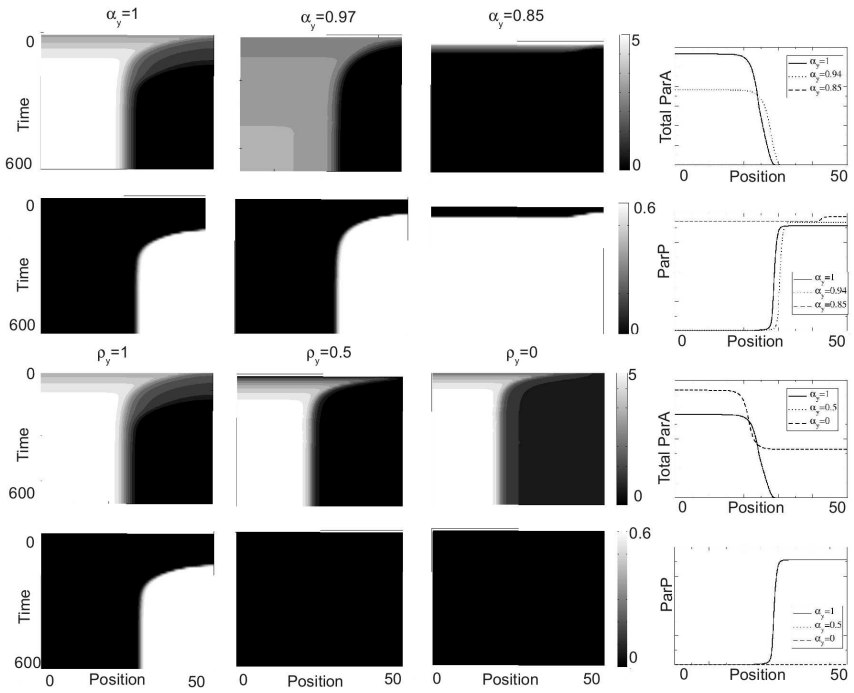

Figure S3: Par protein dynamics coupled to actin model (Tostevin and Howard, 2008) also lose distinct Par domains when cytoplasmic ParA is depleted (top two rows). When ParP is depleted, ParA is still segregated toward the anterior pole (bottom two rows). The first and third rows show ParA levels while the second and fourth rows show ParP levels, for the values of α_y and ρ_y indicated. The right column shows the final profile for each value of α_y or ρ_y for easier comparison of the boundary between the Par protein domains. Both α_y and ρ_y are lowered below levels predicted to result in a loss of bistability in the Par protein dynamics (Figure 5).

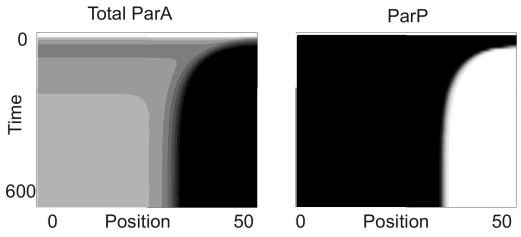

Figure S4: Distinct Par protein domains can be rescued by lowering both ParA and ParP cytoplasmic levels even when coupled to a model of actomyosin dynamics. Here cytoplasmic ParA is lowered well below the level that results in a loss of polarization ($\alpha_y = 0.85$, see Figure S3) and lowering ParP ($\rho_y = 0.8$) allows the model to successfully polarize, consistent with the model of Par protein dynamics alone (Figure 5). Colormap legend is shown in Figure S3.